J Electr Eng Technol.2015; 10(3): 952-957
http://dx.doi.org/10.5370/JEET.2015.10.3.952

ISSN(Print) 1975-0102
ISSN(Online) 2093-7423

Air-Barrier Width Prediction of Interior Permanent Magnet Motor for Electric Vehicle Considering Fatigue Failure by Centrifugal Force

Sung-Jin Kim*, Sang-Yong Jung and Yong-Jae Kim†**

Abstract – Recently, the interior permanent magnet (IPM) motors for electric vehicle (EV) traction motor are being extensively researched because of its high energy density and high efficiency. The traction motor for EV requires high power and high efficiency at the wide driving region. Therefore, it is essential to fully consider the characteristics of the motor from low speed to high-speed driving regions. Especially, when the motor is driven at high speed, a significant centrifugal force is applied to the rotor. Thus, the rotor must be stably structured and be fully endured at the critical speed. In this paper, aims to examine the characteristics of the IPM motor by adjusting the width of air-barrier according to the permanent magnet position which is critical in designing an IPM motor for EV traction motors and to conduct a centrifugal force analysis for grasping mechanical safety.

Keywords: Interior permanent magnet motor, EV traction motor, Air-barrier, Cogging torque, Torque ripple, Electromagnetic field analysis, Centrifugal force analysis, 2-D numerical analysis

1. Introduction

Due to the recent exhaustion of fossil fuels and the strict environmental regulation, new methods of developing vehicles for the future have been widely studied to replace conventional engine driving methods. Therefore, the hybrid electric vehicle (HEV), the electric vehicle (EV), and the plug-in hybrid electric vehicle (PHEV) have been developed in order to replace the conventional diesel-powered or gasoline-powered vehicles that are the major cause of air pollution. The HEVs are already marketed for sale. The performance requirements of the EV traction motors include high torque, high speed, high power, high efficiency and miniaturization [1, 2]. In the permanent magnet (PM) motor for EVs traction, the magnetic flux of field does not depend on external power, but is supplied by means of the PM of a rotor. Therefore, its efficiency and output density is high in comparison with other motors, and it can implement high efficiency and miniaturization. It is increasingly used in each field of the industry [3, 4]. As development of power electronics advances control technology, control motors by vector control are applied to more fields to contribute to popularity thereof for precise control, for example, small AC servo motors.

For this reason, the control system had become simplified along with the development of control technology and the price of rare earth magnets with high energy density like Nd-Fe-B, which was expensive, had dropped and thus become competitive. Furthermore, the problem of impossible self-starting, which had been the biggest weakness of synchronous motor, was resolved by magnetic pole position detection and improved control performance, to the extent that even micro speed control became possible. On the other hand, because the rotor of a motor is connected directly to the mechanical load rotating at high speed, stable stress distribution is essential and it should be designed to fully tolerate critical speed [5-9]. Therefore, an important technology is the structural design of the motor. When designing the structure of a rotor, the width of air-barrier depending on the magnet position affects the operation characteristics of the motor. The wider width of air-barrier makes the centerpost narrower to let the magnetic flux by means of the magnet of rotor not stay in the rotor and send it in the air gap direction to improve torque. However, because the wider width of air-barrier contributes to narrowing the centerpost, the centerpost may be broken by centrifugal force in driving the motor at high speed [10-12]. In this paper, aims to examine the relation by adjusting the width of air-barrier which affects the operation characteristics of the IPM motor and the resulting characteristics of the motor by using the finite element method (FEM) based on 2-D numerical analysis. Moreover, the centrifugal force analysis is conducted to identify an sufficient safety factor of the centerpost is ensured and the structural safety of the IPM motor is also ensured if the width of air-barrier is widened to make a narrow centerpost.

† Corresponding Author: Dept. of Electrical Engineering, Chosun University, Korea. (kimyj21@chosun.ac.kr)
* Dept. of Electrical Engineering, Chosun University, Korea. (kimsj 641@chosun.kr)
** School of Information and Communication Engineering, Sungkyunkwan University, Korea. (syjung@skku.edu)
Received: March 31, 2014; Accepted: November 18, 2014

2. Shape and Specifications of IPM Motor

The specification of the IPM motor for the 2-D numerical analysis is shown in Table 1. The IPM motor for

Table 1. Specifications of IPM motor

Parameter			Value (Unit)
Rotor	Magnet type		Nd-Fe-B
	Number of poles		8 (Poles)
	Silicon steel	Material	35PN230
		Thickness	0.35 (mm)
		Yield point	393 (Mpa)
Stator	Phase		3
	Number of slots		36
	Winding		Distributed
	Silicon steel	Material	35PN230
		Thickness	0.35 (mm)
Maximum speed			14500 (rpm)

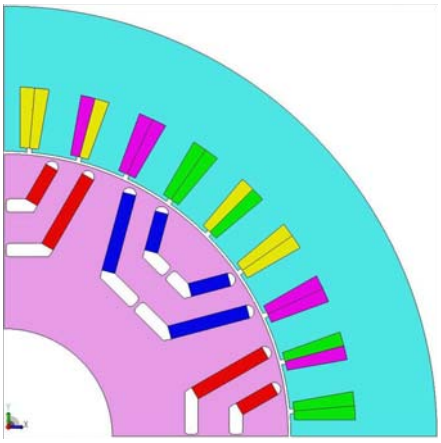

Fig. 1. The cross-sectional diagram of IPM motor

EV traction motors requires high starting torque as well as driving performance of wide speed region. As the IPM motor for EV traction motors implements higher driving speed regions, motors with a driving speed faster than 18000 rpm have been developed. In this study, a motor with a maximum speed of 14500 rpm is selected to establish the maximum speed as a speed based on loading for the centrifugal force analysis in order to draw the width of air-barrier to ensure structural safety. The cross-sectional diagram of the IPM motor for the 2-D numerical analysis is shown in Fig. 1.

As shown in Fig. 2, the air-barrier in the IPM motor is a hole for cooling which also functions as a flux barrier that interrupts the flow of the magnetic flux. Also, the design parameters for an air-barrier of the IPM motor for driving EV traction motors are shown in Fig. 2. The design parameter X_1 and X_3 represent the width of air-barrier, and X_2 is the width of the centerpost.

The IPM motor must be designed so that sufficient magnetic saturation can be achieved for the centerpost or the bridge part to maximize the reluctance torque. This is intended to reduce the magnetic flux through the centerpost or the bridge when the magnetic saturation is done so that the magnetic flux generated by the magnet of rotor can be sent to the stator [13]. For sufficient magnetic saturation of the centerpost, the width of air-barrier must be wide. However, when the width of air-barrier is wide, the

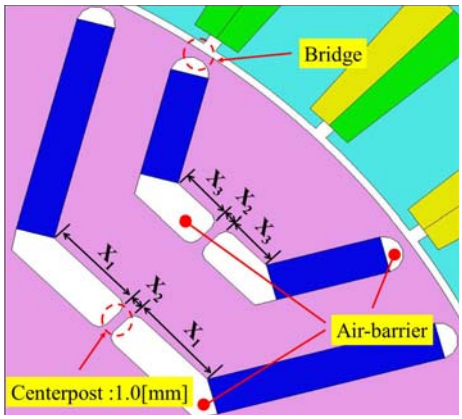

Fig. 2. Design parameters of air-barrier

Table 2. Design parameters

		X_1(mm)	X_2(mm)	X_3(mm)
Basic model		9.9	1.0	5.5
Adjustment model	I	10.0	0.8	5.6
	II	10.1	0.6	5.7
	III	10.2	0.4	5.8
	IV	10.3	0.2	5.9

centerpost is narrowed to result in the risk of damaging the centerpost in high speed driving. Thus, it is necessary to grasp the width of air-barrier in consideration of the fatigue strength of the material of rotor core. Table 2 shows the design parameters for the basic model and the model for adjusting the width of air-barrier. As shown in Table 2, the electromagnetic field analysis and the centrifugal force analysis was conducted by adjusting the air-barrier width of basic model from 9.9 mm up to 10.3 mm at the intervals of 0.1 mm to grasp the structural limit width of air-barrier.

3. Electromagnetic Field Analysis of IPM Motor by Adjusting Width of Air-Barrier

Fig. 3 shows the magnetic flux density distribution. Fig. 3(a) shows the magnetic flux density distribution of the basic model with the air-barrier width of 9.9 mm, while Fig. 3(b) shows the magnetic flux density distribution of the adjustment model IV with the air-barrier width of 10.3 mm.

As shown in Fig. 3, the wider width of air-barrier contributes to the severer saturation of magnetic flux at the centerpost. The basic model has the maximum magnetic flux density of 2.10 T but the adjustment model IV has 2.31 T.

3.1 Cogging torque

Fig. 4 shows the cogging torque changes according to the width of air-barrier. The combination of both the number of poles and the number of slots contributes to repeating waveforms at each mechanical angle 5 deg.

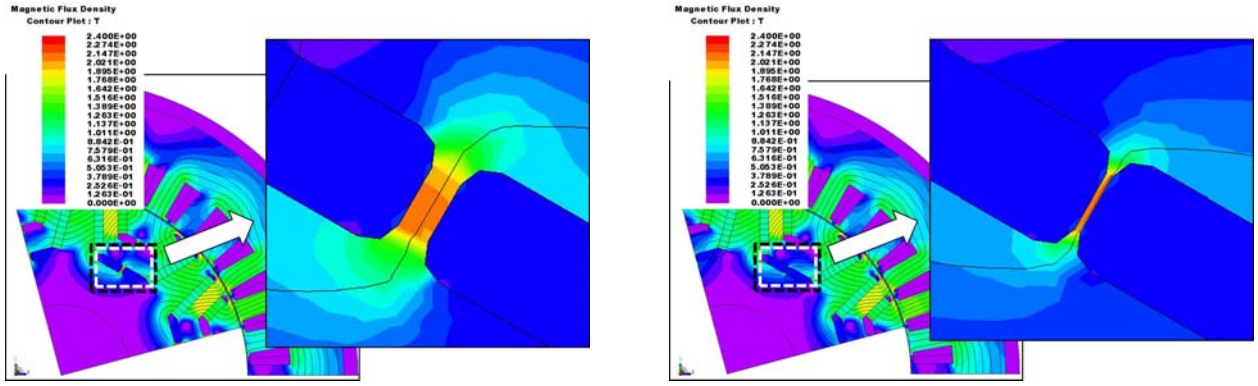

(a) (b)

Fig. 3. Magnetic flux density distribution: (a) Basic model; (b) Adjustment model IV.

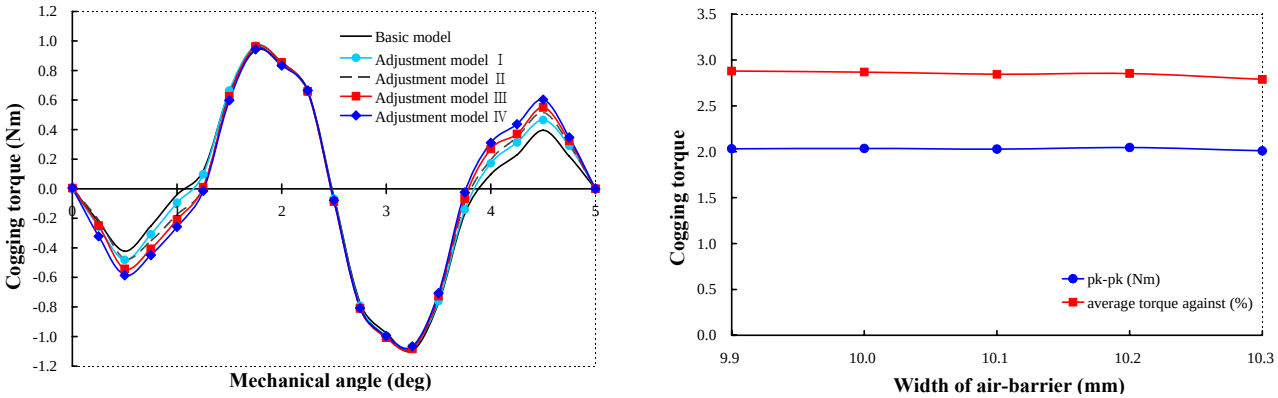

(a) (b)

Fig. 4. Cogging torque changes according to the width of air-barrier: (a) Cogging torque waveforms; (b) pk-pk and the average torque against of cogging torque.

The cogging torque waveforms according to the width of air-barrier are shown in Fig. 4(a), and Fig. 4(b) shows the cogging torque pk-pk and the average torque against. As shown in Fig. 4, the maximum of cogging torque of the basic model is 0.94 Nm, and the maximum of the adjustment model IV is 0.94 Nm. Hereby, it was confirmed that adjusting the width of air-barrier does not change the cogging torque.

3.2 Torque

Fig. 5 shows torque changes according to the width of air-barrier at the maximum speed of 14500 rpm. Fig. 5(a) shows the torque waveforms according to the width of air-barrier. Fig. 5(b) shows both the average and maximum torques according to the width of air-barrier, and Fig. 5(c) shows the torque ripple according to the width of air-barrier. As shown in Fig. 5, the wider the width of air-barrier, average torques and maximum torques are increased.

As a result of Adjusting the width of air-barrier from 9.9 mm to 10.3 mm, the maximum torque and the average torque increased by about 1.54 Nm, 1.47 Nm, respectively. In the basic model, the torque ripple was generated by 10.32 %. However, in the adjustment model IV with the adjusted width of air-barrier of 10.3 mm, it is 10.29 % reduced by 0.03 %. From the result above, it is observed that the wider width of air-barrier results in torque increases but torque ripple decreases.

4. Centrifugal Force Analysis of IPM Motor by Adjusting Width of Air-barrier

In order to examine the structural safety of the IPM motor at maximum speed driving, the centrifugal force analysis was conducted by using each model of which the width of air-barrier where the maximum torque occurs was adjusted. The centrifugal force analysis was conducted in the static load condition while driving the motor constantly at the maximum speed of 14500 rpm in consideration of the material properties values.

In this analysis, Von Mises stress is applied. The centrifugal force is proportional to square of rotating speed as shown in (1),

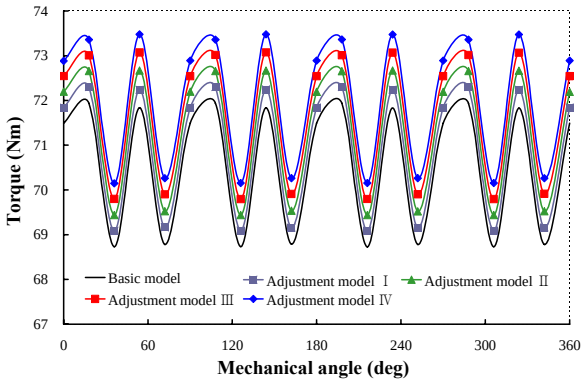

(a)

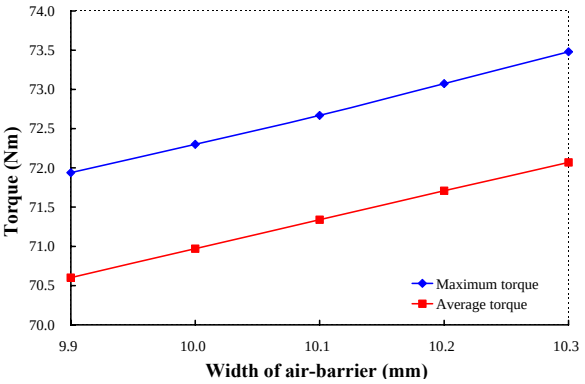

(b)

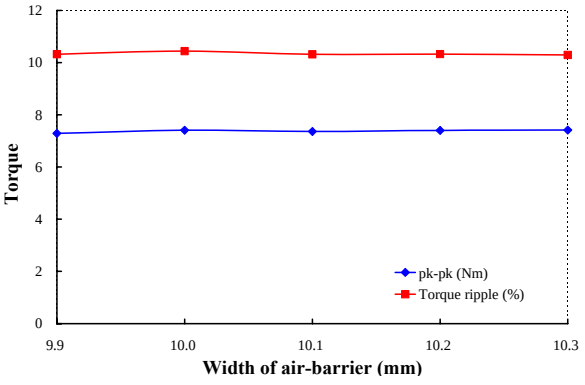

(c)

Fig. 5. Torque changes according to the width of air-barrier at maximum speed of 14500 rpm: (a) Torque waveforms; (b) Average and maximum torques; (c) Torque ripple.

$$F = mv^2/r \tag{1}$$

where, F is centrifugal force, m is mass, v is rotating speed and r is radius of rotor. Centrifugal force is proportional to square of speed [14]. Therefore, it is necessary to calculate the mechanical stress caused by centrifugal force at high speed. Fig. 6 shows the stress distribution of the IPM motor obtained through the centrifugal force analysis. Fig. 6(a) shows the stress distribution of the basic model with the air-barrier width of 9.9 mm. The stress distribution of the adjustment model IV with the air-barrier width of 10.3 mm is shown in Fig. 6(b).

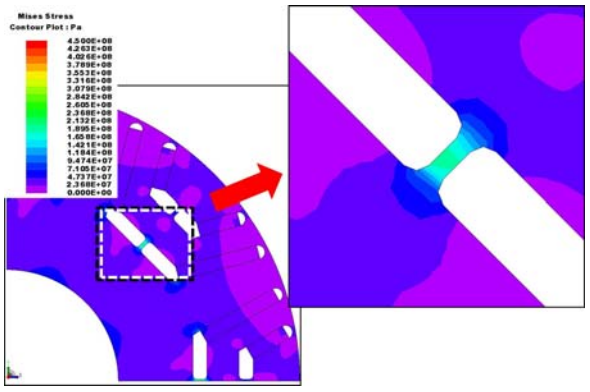

(a)

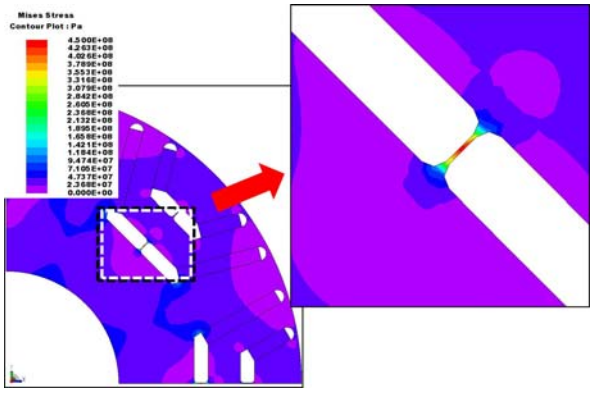

(b)

Fig. 6. Stress distribution of IPM motor at the maximum speed of 14500 rpm: (a) Basic model; (b) Adjustment model IV.

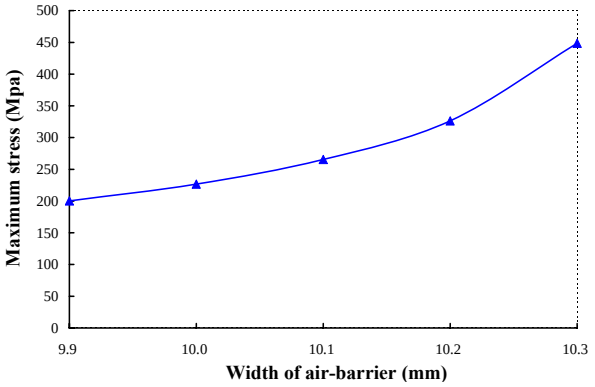

Fig. 7. Maximum stress of each model.

As shown in Fig. 6, the stress is concentrated on the centerpost.

The maximum stress according to the width of air-barrier is shown in Fig. 7. As shown in Fig. 7, the maximum stress value of adjustment model IV with the width of air-barrier of 10.3 mm is about 448.580 Mpa. This value which is greater than the yield point 393 Mpa of silicon steel (35PN230) for the rotor, and the rotor may be broken during high speed driving in this case. The safety factor

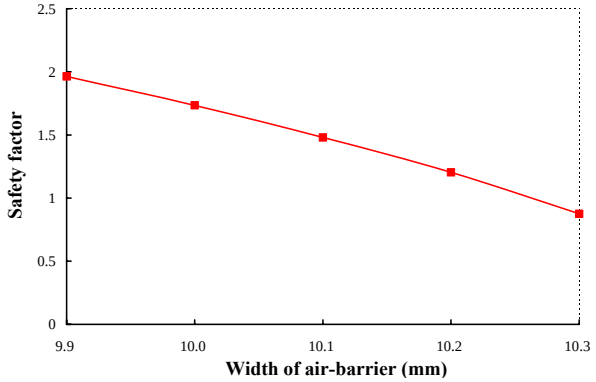

Fig. 8. Safety factor of each model.

according to the width of air-barrier is shown in Fig. 8. The safety factor is 0.87 even smaller than the safety factor of stable general electrical machinery. Therefore, it is ideal to select the adjustment model IV of which the width of air-barrier is 10.3 mm in consideration of just the electromagnetic characteristics. However, if the structural characteristics are considered as well, it is ideal to select the width of air-barrier under than 10.2 mm to implement an ideal safety factor between 1.3 and 1.5. Although it is not described in this paper, an analysis was conducted on the dynamic load condition according to the operating and static testing for the motor durability test.

5. Conclusion

This paper has presented the electromagnetic field analysis and the centrifugal force analysis according to the width of air-barrier in the high speed driving region of the IPM motor for EV traction motors by using the FEM based on 2-D numerical analysis. As the electromagnetic field analysis result, it was confirmed that more improved operation characteristics of the IPM motor are achieved with the wider width of air-barrier. The cogging torque does not have a significant effect on the width of air-barrier. However, both the average and maximum torques increased by approximately 2 % by adjusting the width of air-barrier. Moreover, the torque ripple which adversely affects the driving characteristics of the IPM motor decreases as the width of air-barrier is wider. Also, the structural limit width of the air-barrier is identified through the centrifugal force analysis. By integrating the result of this study with the optimum design, a more improved and advanced design technology for the IPM motors will be established to ensure the resulting stability as well.

Acknowledgements

This work was supported by the Human Resources Program in Energy Technology of the Korea Institute of Energy Technology Evaluation and Planning (KETEP), granted financial resource from the Ministry of Trade, Industry & Energy, Republic of Korea. (No. 20134010200550).

References

[1] K. Yamazaki, H. Ishigami, "Rotor-Shape Optimization of Interior-Permanent-Magnet Motors to Reduce Harmonic Iron Losses", *IEEE Trans. Ind. Electron.*, vol.57, no.1, pp.61-69, Jan. 2010.

[2] D. Pavlik, V. K. Garg, J. R. Repp, J. Weiss, "A Finite Element Technique for Calculating the Magnet Sizes & Inductances of Permanent Magnet Machine", *IEEE Trans. Energy Conv.*, vol. 3, no. 1, pp. 116-122, Mar. 1998.

[3] Fei Zhao, Lipo T. A, Byung-Il Kwon, "A Novel Two-Phase Permanent Magnet Synchronous Motor Modeling for Torque Ripple Minimization", *IEEE Trans. Magn.*, vol. 49, no. 5, pp. 2355-2358, May 2013.

[4] J. K. Kim, S. Y. Kwak, S. M Cho, H. K. Jung, T. K. Jung, and S. Y. Jung "Optimization of Multilayer Buried Magnet Synchronous Machine Combined With Stress and Thermal Analysis," *IEEE Trans. Magn.*, vol. 42, no. 4, pp. 1023-1026, Apr. 2006.

[5] Yoshinari Asano, Yukio Honda, Yoji Takeda, Shigeo Morimoto, "Reduction of Vibration on Concentrated Winding Permanent Magnet Synchronous Motors with Considering Radial Stress", *Trans. IEE Japan*, vol. 121, no. 11, pp. 1185-1191, 2001.

[6] B. Sneyers, D. W. Novotny and T. A. Lipo, "Field weakening in buried permanent magnet ac motor drives", *IEEE Trans. Ind. Appl.*, vol. 21, no. 2, pp. 398-407, Mar. 1985.

[7] P. M. Lindh, H. K. Jussila, M. Niemela, A. Parviainen, and J. Pyrhonen, "Comparison of concentrated winding permanent magnet motors with embedded and surface-mounted rotor magnets," *IEEE Trans. Magn.*, vol. 45, no. 5, pp. 2085-2089, May 2009.

[8] Sang-Yeop Kwak, Jae-Kwang Kim, Hyun-Kyo Jung, "Characteristic Analysis of Multilayer-Buried Magnet Synchronous Motor Using Fixed Permeability Method", *IEEE Trans. Energy Conv.*, vol. 20, no. 3, pp. 549-555, Sept. 2005.

[9] Z. Q. Zhu, David Howe, "Influence of Design Parameter on Cogging Torque in Permanent Magnet Machines", *IEEE Trans. Energy Conv.*, vol. 15, no. 4, Dec. 2000.

[10] Gulez K., Adam A.A., Pastaci H., "A Novel Direct Torque Control Algorithm for IPMSM With Minimum Harmonics and Torque Ripples", *IEEE/ASME Trans. Mechatron.*, vol. 12, no. 2, pp. 223-227, Apr. 2007.

[11] E. C. Lovelace, T. M. Jahns, "Mechanical Design Considerations for Conventionally-laminated, High-Speed, Interior PM Synchronous Machine Rotors", *IEEE Trans. Ind. Appl.*, vol. 40, no. 3, pp. 806-812, May 2004.

[12] Seungho Lee, Yu-Seok Jeong, Yong-Jae Kim, Sang-Yong Jung, "Novel Analysis and Design Methodology of Interior Permanent-Magnet Synchronous Motor Using Newly Adopted Synthetic Flux Linkage", *IEEE Trans. Ind. Electron.*, vol. 58, no. 9, pp. 3806-3814, Sept. 2011.
[13] Ho-Kyoung Lim, Baik-Kee Song, Sung-Il Kim, Jung-Pyo Hong, "A Study on the Relation Between Rotor Rib and Maximum Power of IPMSM in Flux Weakening Region", *in Conf. 2010 ICEMS Int. Conf. Electrical Machines and System*, pp.1222-1225, 2010.
[14] Jae-Woo Jung, Byeong-Hwa Lee, Do-Jin Kim, Jung-Pyo Hong, Jae-Young Kim, Seong-Min Jeon, Do-Hoon Song, "Mechanical Stress Reduction of Rotor Core of Interior Permanent Magnet Synchronous Motor", *IEEE Trans. Magn.*, vol. 48, no. 2, pp. 911-914, Feb. 2012.
[15] Chan-Bae Park, Byung-Song Lee and Hyung-Woo Lee, "Performance Comparison of the Railway Traction IPM Motors between Concentrated Winding and Distributed Winding", *J. Elect. Eng. Technol.*, vol. 8, no. 1, pp. 118-123, 2013.
[16] Cheol-Min Kim, Dong-Yeong-Kim, Gyu-Won Cho and Gyu-Tak Kim, "The Design of Flux Barrier for Improvement of Demagnetization Endurance in BLDC Motor", *J. Elect. Eng. Technol.*, vol. 9, no. 6, pp. 2182-2186, 2014.

Sung-Jin Kim He received B.S and M.S degree in department of electrical engineering from Chosun University, Gwang-ju, Korea in 2011 and 2013, respectively. Since 2013, he's doing a Ph.D course in department of electrical engineering from Chosun University, Gwang-ju, Korea. His research interests are numerical analysis and design of linear machineries and PM machineries.

Sang-Yong Jung He received the B.S., M.S., and Ph.D. degrees in electrical engineering from Seoul National University, Seoul, Korea, in 1997, 1999, and 2003, respectively. From 2003 to 2006, he was a Senior Research Engineer with the R&D Division, Hyundai Motor Company, Korea, and the R&D Division, Kia Motor, Korea. From 2006 to 2011, he was an Assistant Professor with the Department of Electrical Engineering, Dong-A University, Busan, Korea. He is currently an Associate Professor with the School of Information and Communication Engineering, Sungkyunkwan University, Suwon, Korea. His research interests include the numerical analysis and optimal design of electric machines and power apparatus.

Yong-Jae Kim He received B.S degree in department of electrical engineering from Chosun University, Gwang-ju, Korea in 1996 and the M.S, Ph.D degree in electrical engineering from Musashi Institute of Technology, Tokyo, Japan in 2003 and 2006, respectively. From 2006 to 2007, he was a Researcher of electrical and electronic engineering with the Musashi Institute of Technology, Tokyo, Japan. He is currently an Associate Professor with the Department of Electrical Engineering, Chosun University, Gwangju, Korea. His current research interests include the design and analysis of electric machines.